Alterations in lipoprotein composition associated with galactosamine-induced rat liver injury

Charles K. Cartwright, James B. Ragland, Stuart W. Weidman, and Seymour M. Sabesin

Division of Gastroenterology, Department of Medicine, University of Tennessee Center for the Health Sciences, Memphis, TN 38163

Abstract The apoprotein and lipid composition and the morphology of lipoproteins was determined in rats with D-(+)-galactosamine (GalN) hepatitis. Single intraperitoneal injections of GalN at several dose levels and postinjection exsanguination times resulted in depressed levels of cholesteryl esters, an index of plasma lecithin:cholesterol acyltransferase (LCAT) activity, and increased levels of phospholipids, unesterified cholesterol, and triglycerides. Plasma withdrawn from rats 24 hr after injection of 1000 mg/kg GalN was most deficient in cholesteryl ester and was studied further by sequential isolation of VLDL, LDL, HDL_1, HDL_2, and HDL_3. The increased plasma triglyceride (TG) after GalN treatment accumulated in TG-rich VLDL which contained two types of particles: a large (mean diameter 193.6 ± 48.3 nm) and rough-edged particle, and a smooth one with a mean diameter (63.4 ± 13.2 nm) similar to control VLDL (69.4 ± 20.2 nm). The increased phospholipids and unesterified cholesterol were predominantly in LDL, HDL_1, and HDL_2 which were largely rouleaux of flattened vesicles. Density gradient ultracentrifugation of $d > 1.006$ g/ml lipoproteins confirmed these results. GalN hepatitis appeared to decrease the larger $apoB_{335K}$ subspecies and the apoC-III_0 and apoC-III_2 content of VLDL. However, total apoB concentration as GalN VLDL was increased 2.6-fold over control. LDL and HDL were markedly enriched in apoE. LDL apoB concentration was decreased by 41% while HDL was deficient in apoA-I, A-II and A-IV, and C. These results demonstrate association of increased plasma triglycerides with particles of grossly abnormal apoprotein composition, and the association of increased plasma phospholipids and unesterified cholesterol with apoE-rich lipoproteins during the LCAT defect produced by GalN hepatitis. These abnormal lipoproteins may represent an abnormal level of normal LCAT substrates important in the transport and esterification of plasma cholesterol.—**Cartwright, C. K., J. B. Ragland, S. W. Weidman, and S. M. Sabesin.** Alterations in lipoprotein composition associated with galactosamine-induced rat liver injury. *J. Lipid Res.* 1982. **23:** 667–679.

Supplementary key words apoA-I • apoB • apoE • apoC • lecithin:cholesterol acyltransferase • VLDL • LDL • HDL • density gradient ultracentrifugation

The formation of plasma lipoproteins is dependent upon the metabolism of precursor (nascent) lipoproteins secreted from the liver or intestine (1). The conversion of nascent to mature lipoproteins involves enzymatic modifications of lipids by lipoprotein lipase, hepatic lipase, and lecithin:cholesterol acyltransferase (LCAT), and the exchange of apoproteins and lipids with other lipoproteins and cells.

One nascent lipoprotein synthesized by the liver is nascent high density lipoprotein (HDL) which is different in composition and structure from HDL found in normal plasma (2). Nascent HDL, isolated from rat liver perfusates, consists primarily of apolipoprotein E (apoE), phospholipid, and unesterified cholesterol (3) in contrast to circulating HDL composed predominantly of apolipoprotein A-I (apoA-I) and cholesteryl ester (4). When the nascent HDL particles are negatively stained they appear by electron microscopy as disc-shaped particles (45 Å thick and 200 Å diameter) in contrast to the spherical particles (80–100 Å diameter) of HDL in plasma. Recent studies have shown that over 50% of the apoA-I and much of the phospholipid of plasma HDL originates in the intestine, while over 99% of the apoE of plasma HDL is of hepatic origin (1, 5).

Hamilton et al. (6) have proposed that either LCAT, secreted by the liver, or a complex of LCAT and apoA-I utilizes nascent HDL as a substrate for the formation of cholesteryl esters, thereby transforming the bilamellar discs into spherical particles. Indirect evidence in support of this concept is the enrichment in discoidal HDL induced by the presence in liver perfusates of a potent LCAT inhibitor, 5,5′-dithiobisnitrobenzoic acid (DTNB).

Previous studies by Ragland and co-workers (7, 8) have demonstrated abnormal HDL in the plasma of patients with alcoholic hepatitis who have LCAT deficiency due to hepatocellular injury. The HDL in alcoholic hepatitis is enriched in unesterified cholesterol, in phospholipid, and apoE, decreased in apoA-I, and appears as chains of discoidal particles when negatively stained for electron microscopy. Marcel et al. (9) and

Abbreviations: HDL, high density lipoprotein; LDL, low density lipoprotein; VLDL, very low density lipoprotein; LCAT, lecithin:cholesterol acyltransferase; GalN, galactosamine; PAGE, polyacrylamide gel electrophoresis; DTNB, 5,5′-dithiobisnitrobenzoic acid; apo, apolipoprotein; SDS, sodium dodecyl sulfate; TMU, tetramethyl urea.

Mitchell et al. (10), using affinity chromatography techniques, have recently reported the isolation of similar apoE-enriched discoidal HDL from patients with alcoholic hepatitis and familial LCAT deficiency, respectively. It has been proposed that this discoidal HDL represents the in vivo accumulation of nascent HDL and provides the principal pathway by which apoE is secreted by the liver in man (8); however, the quantitative contribution of apoE in nascent VLDL to total plasma apoE levels remains to be determined.

Alcoholic hepatitis results in plasma LCAT deficiency (11) and the abnormal lipoproteins in these patients are similar to those in LCAT-deficient rats treated with GalN (12, 13). Twenty-four hr after a single injection of GalN, plasma LCAT activity is depressed, cholesteryl esters are reduced, and discoidal LDL and HDL accumulate in plasma. The abnormalities in plasma lipid and lipoprotein composition produced by GalN have been attributed to the decreased LCAT activity and concomitant defects in lipoprotein metabolism. To further understand the lipoprotein abnormalities that occur in the presence of LCAT deficiency, we have performed a detailed analytical and ultrastructural study of plasma lipoproteins isolated by both sequential and density gradient ultracentrifugation from rat plasma 24 hr after GalN administration and have correlated the morphology of these lipoproteins with their composition. These results provide an insight into the composition and morphology of lipoproteins whose metabolic transformation by LCAT may normally occur only transiently after secretion.

MATERIALS AND METHODS

Animals

Female Sprague-Dawley rats, (Southern Animal Farms, Pratteville, AL) weighing 175–200 g were used in all experiments. Animals fasted for 4–6 hr were given a single intraperitoneal injection of D-(+)-galactosamine HCl (Sigma Chemical Co., St. Louis, MO) in normal saline. Experimental animals were injected with 750, 1000, and 1250 mg of GalN/kg body weight in 0.5–1.0 ml of saline. Control animals were injected with saline. Both control and experimental animals had access to water, but not food, for the remainder of the experiment. At 24 and 36 hr after injection animals were exsanguinated by abdominal aortic puncture. Blood was drawn into tubes containing EDTA (0.03 μM) and DTNB (1 μM) and plasma was separated by centrifugation at 5°C. Because of variability in the severity of the hepatitis produced by GalN, each plasma was analyzed before being pooled. Samples were analyzed for total and free cholesterol, triglyceride, and phospholipid, and lipoproteins were determined by agarose electrophoresis. The livers were examined grossly for fat accumulation and were removed for histological examination.

Homogeneity of lipoproteins in pooled plasma samples was improved by using only plasma from animals with marked deficiency in cholesteryl esters (<15% of total cholesterol in esterified form), total absence of an α-lipoprotein electrophoretic band, and grossly fatty livers.

Lipoprotein separations

Plasma lipoproteins were fractionated at 17°C by sequential ultracentrifugation as described by Lindgren (14) using a Beckman TI 50 rotor and the following density ranges: VLDL, $d < 1.006$ g/ml (178×10^6 g-min); LDL, $1.006 < d < 1.050$ g/ml (483×10^6 g-min); HDL_1, $1.050 < d < 1.070$ g/ml (483×10^6 g-min); HDL_2, $1.070 < d < 1.125$ g/ml (483×10^6 g-min); and HDL_3, $1.1125 < d < 1.210$ g/ml (483×10^6 g-min). Since GalN hepatitis is produced in fasting animals, a chylomicron fraction was not isolated. All lipoprotein fractions were washed by ultracentrifugal flotation through two volumes of overlay solution of the appropriate density and washed fractions were dialyzed overnight against dilute EDTA solutions containing 0.02% sodium azide. All analyses were performed immediately following lipoprotein separation and dialysis.

Density gradient centrifugation of $d > 1.006$ g/ml lipoproteins (LDL and HDL) was carried out as follows. Control and experimental plasmas were centrifuged for 178×10^6 g-min in a Beckman SW 50.1 rotor. The $d < 1.006$ g/ml lipoproteins were removed by tube slicing and 2 ml of the infranatant was adjusted to $d = 1.240$ g/ml with solid sodium bromide and sucrose. These solutions were then overlaid with an exponential density gradient from $d = 1.229$ to 1.006 g/ml. Blank gradients were overlaid over salt-sucrose solutions ($d = 1.240$ g/ml) and all gradients were spun in a Beckman SW 41 rotor for 295×10^6 g-min at 17°C. After centrifugation, gradients were fractionated through an Isco (Instrumentation Specialties Co., Lincoln, NE) density gradient fractionator and fraction densities were measured with a Newtec (Newtec Inc., Birmingham, AL) high precision digital densitometer.

Initially gradients were spun for 295×10^6 g-min, 444×10^6 g-min, and 592×10^6 g-min to determine centrifugation equilibrium conditions. At 295×10^6 g-min, distribution of lipoproteins in centrifugal density gradients did not differ from that in gradients spun longer.

Quantitative analysis of lipids and apolipoproteins

Plasma and lipoprotein triglycerides were determined by the method of Biggs, Erickson, and Moorehead (15). Cholesterol and cholesteryl esters were determined by

gas–liquid chromatographic analysis of extracts of saponified and nonsaponified samples, and esterified cholesterol was estimated by difference (16). Cholesteryl ester values were calculated from cholesterol determinations using a correction factor of 1.67. An internal standard of β-sitosterol was added to each sample prior to extraction and was used as a basis for the calculation of results. Plasma and lipoprotein phospholipids were determined by extraction of samples by sequential addition of 50 vol of methanol and 50 vol of chloroform. Extracts were dried under nitrogen, digested with 70% perchloric acid, and phosphorus was determined by the method of Rouser, Fleischer, and Yamamoto (17). Phosphorus values were converted to phospholipid values using a factor of 25.

Density gradient fractions were also assayed for unesterified cholesterol, cholesteryl ester, and phospholipid. Based on analysis of whole plasma pools and $d > 1.006$ g/ml fractions, the calculated gradient recoveries ranged from 96% to 112%. The results of gradient analysis, corrected for dilution, are represented as plasma levels.

Total protein was determined by the method of Markwell et al. (18). Agarose electrophoresis was performed using the apparatus and method supplied by Corning-ACI (Corning-ACI, Palo Alto, CA) and stained with fat red 7B.

Discontinuous polyacrylamide slab gel electrophoresis (PAGE) was carried out according to the method of Laemmli (19). In some experiments 2-mercaptoethanol was omitted from apoprotein solubilizing buffer. Stacking gels (pH 6.8) were 3% polyacrylamide and the running gel (pH 8.8) was a linear gradient from 10 to 20% or 3.5 to 27% polyacrylamide. Electrophoresis was performed immediately after formation of the stacking gel in a Hoefer (Hoefer Scientific Co., San Francisco, CA) vertical slab apparatus, and gels were fixed, stained, and destained with solutions described by Weber and Osborne (20). Apolipoprotein B (apoB) was quantified by the isopropyl alcohol method of Holmquist, Carlson, and Carlson (21). All sequentially isolated lipoproteins were analyzed for apoprotein content using 25 μg of apoprotein, whereas equal volumes (35 μl) of density gradient fractions were used to determine apoprotein content of density gradient fractions.

Identification of lipoprotein apoproteins was based on the migration of molecular weight standards and on the identical migration of purified apoprotein (apoA-I) prepared by standard methods (22). Analytical isoelectric focusing (IEF) was performed according to the method of Weidman et al. (23). In each case 50 μg of lipoprotein apoproteins was subjected to isoelectric focusing procedures. Identification of bands in IEF gels was based on their isoelectric point and identity with IEF patterns of Swaney and Gidez (24).

Based on the results of lipoprotein analysis, hydrated densities were calculated using a weighted summation of individual component densities. Density values for the individual components were assumed to be 1.30 for apolipoprotein, 1.967 for cholesterol, 0.909 for cholesteryl ester, 0.915 for triglyceride, and 1.030 for phospholipid.

Electron microscopy

Samples for electron microscopy were dialyzed against 1mM EDTA, 0.01% sodium azide, pH 7.6. Lipoproteins were negatively stained for electron microscopy with phosphotungstate solutions (pH 5.9) as described by Forte and Nichols (25). To insure uniformity in morphological analysis of density gradient fractions, lipoproteins were floated on formvar-coated grids from equal fraction volumes for 3 sec. Negative staining was then carried out for 2 min in an identical manner for all fractions. Particle size was determined with a magnifying micrometer. In each preparation the diameters of 100 free-standing spherical particles were measured. In each preparation containing discoidal particles the edge thickness and long-axis of 100 particles was measured.

RESULTS

Effects of galactosamine on plasma lipids

Our initial aim was to determine the optimal conditions for performing analytical studies of the abnormal lipoproteins in GalN hepatitis. Dose and time experiments determined conditions of maximal depression of plasma cholesterol esterification with maintenance of sufficient cholesterol to allow detailed lipoprotein characterization. The effects of three doses of GalN on plasma lipids were evaluated at 24 and 36 hr after injection since the GalN hepatic injury is maximal at those times (26). Rats were fasted throughout the experiment since feeding prevents development of hepatitis and lipoprotein alterations (27).

GalN at 750, 1000, or 1250 mg/kg produced significant alterations in plasma lipids (**Table 1**). Total cholesterol decreased by an average of 57%, due mainly to decreased cholesteryl esters (Table 1). Unesterified cholesterol in GalN-treated groups was moderately increased while cholesteryl esters were depressed from 68.8 to 88.9% (Table 1). Increased phospholipids (39.2%) in the GalN-treated groups strongly correlated with increased unesterified cholesterol levels ($r > 0.95$).

The lowest plasma cholesteryl esters were produced by 1000 mg/kg GalN and exsanguination 24 hr after injection (Table 1). Under these conditions, mean cholesteryl ester values were 6.94 mg/dl. Since the response to GalN is variable, only plasma from GalN-treated

TABLE 1. Effect of D-(+)-galactosamine (GalN) hepatitis on plasma lipids[a]

GalN	n	Total Cholesterol	Cholesteryl Esters[b]	Free Cholesterol	Phospholipids	Triglycerides
			mg/dl			
Exsanguinated 24 hr after injection						
750 mg/kg	10	42.01 ± 2.47	19.32 ± 1.85	30.43 ± 2.08	206.07 ± 6.38	39.07 ± 3.74
1000 mg/kg	9	30.51 ± 2.95	6.94 ± 0.65	26.36 ± 3.01	182.30 ± 8.13	52.91 ± 1.59
1250 mg/kg	9	35.72 ± 2.46	14.07 ± 1.788	27.29 ± 2.82	187.95 ± 7.11	42.70 ± 3.66
Exsanguinated 36 hr after injection						
750 mg/kg	10	38.04 ± 4.58	15.11 ± 0.99	28.95 ± 4.20	272.71 ± 7.65	35.29 ± 4.00
1000 mg/kg	9	36.02 ± 1.92	11.87 ± 1.35	28.96 ± 1.84	186.51 ± 5.03	50.02 ± 5.14
1250 mg/kg	10	27.01 ± 1.66	9.07 ± 0.95	21.58 ± 1.96	179.72 ± 5.99	39.94 ± 8.01
Control—exsanguinated 24 hr after saline injection						
	20	59.32 ± 6.17	62.20 ± 1.91	22.90 ± 3.71	145.45 ± 2.86	23.08 ± 2.64

[a] Values are the means of individual animals of each treatment group ± SEM.
[b] Calculated from total and free plasma cholesterol determinations assuming a mass ratio of cholesteryl ester to cholesterol of 1.67.

animals (1000 mg/kg GalN for 24 hr), whose cholesterol was less than 15% esterified, was pooled and used for lipoprotein studies.

Histological examination of livers was also used to determine whether the 1000 mg/kg dose level produced greater hepatocellular injury and fatty infiltration than the 750 mg/kg dose level used previously (12). We found no differences in the extent of hepatocellular necrosis or fat accumulation despite the increased dose.

Lipid composition of lipoproteins isolated by sequential ultracentrifugation

The lipid composition of sequentially isolated lipoproteins is shown in **Table 2.** GalN produced a marked increase in the triglyceride content of VLDL which reflected an almost threefold increase in total lipoprotein mass. Table 2 also shows that VLDL cholesteryl esters were decreased (3.8 vs. 6.3% control) while the unesterified cholesterol was elevated (7.8 vs. 5.9% control). Similarly low density lipoprotein (LDL) concentration was increased 43.5% due to increased phospholipid, unesterified cholesterol, and triglyceride, while cholesteryl esters were depleted following GalN.

HDL mass shifts to lower densities with GalN. As shown in Table 2, HDL_1 concentration increased sixfold and HDL_2 mass decreased 34%, while HDL_3 decreased 74%. Thus, GalN induces lower density HDL due to decreased protein and cholesteryl ester and increased phospholipid and unesterified cholesterol. We

TABLE 2. Compositions of lipoprotein fractions isolated by sequential ultracentrifugation

	UC[a]	CE	TG	PL	Prot.	ApoB	Total LP	Calculated Hydrated Density[b]
			% of total			*mg/dl*	*mg/dl*	*g/ml*
VLDL (d 1.006 g/ml)								
GalN	7.8	3.8	57.3	16.7	14.3	0.94	74.3	
Control	5.9	6.3	62.2	12.9	12.7	0.36	27.2	
LDL (d 1.006–1.050 g/ml)								
GalN	25.8	1.7	18.7	37.2	20.2	1.97	34.3	1.037
Control	14.8	18.1	31.6	17.4	22.7	3.36	23.9	1.011
HDL_1 (d 1.050–1.070 g/ml)								
GalN	17.2	2.1	3.7	61.0	15.1	4.47	67.9	1.060
Control	7.8	20.6	12.0	29.1	28.5	2.26	6.3	1.050
HDL_2 (d 1.070–1.125 g/ml)								
GalN	19.8	6.1	4.1	38.0	29.8		40.2	1.082
Control	2.7	20.7	2.0	29.5	36.9		60.7	1.081
HDL_3 (d 1.125–1.210 g/ml)								
GalN	8.7	2.1	0.1	45.9	42.6		22.4	1.139
Control	9.9	15.5	0.3	22.4	51.9		87.3	1.154

[a] UC, unesterified cholesterol; CE, cholesteryl esters; TG, triglycerides; PL, phospholipids; Prot., proteins.
[b] Hydrated density values of 1.30 for apoprotein, 1.067 for cholesterol, 0.909 for cholesteryl ester, 0.915 for triglyceride, and 1.030 for phospholipid were used to calculate density values.

demonstrate this effect on particle hydrated density in Table 2.

Apoprotein composition of sequentially isolated lipoprotein fractions

Marked differences between the apparent apoprotein composition of control and GalN lipoproteins were found by PAGE analysis. Since these lipoproteins were isolated by standard flotation methods and had characteristic lipid compositions and morphologies, we assume that apoproteins in this study were identical to those in other studies. Apoprotein identities in gradient gels used here were based on the molecular weight determined according to the migration of molecular weight standards and purified apoA-I (**Fig. 1C**). We have not determined the chromogenicity of each apoprotein and thus our results provide only a relative index of lipoprotein apoprotein changes. Results of these analyses are shown in photographs of gels (Fig. 1A, 1B, and 1C) and profiles of densitometric scans (Fig. 1D). Equivalent protein from each sequential fraction was electrophoresed, and thus these gels reflect differences in composition rather than in total apoprotein at different densities (see density gradient apoprotein analysis below).

Albumin, apoA-IV, apoE, and apoA-I were well resolved by these gels, but not apoC peptides and apoA-II, which were analyzed by isoelectric focusing. ApoB (Fig. 1B) was determined by the isopropanol precipitation method of Holmquist et al. (21) shown in Table 2.

GalN VLDL was depleted in apoC (Fig. 1A). LDL and HDL (Fig. 1B) were enriched in apoE. Densitometry of stained gels in Fig. 1B showed that the apoE content of LDL appeared similar in both groups though the percent of apoE in these fractions differed due to the presence of other apoproteins (Fig. 1C). Control LDL contained more apoB (3.36 mg control vs. 1.97 mg GalN) while GalN-LDL contained albumin, apoA-I, apoD, and apoC.

Fig. 1A is a 3.5–27% acrylamide gradient slab gel whereas the gel of Fig. 1B is a 10–20% acrylamide gradient. The former gel system resolves the apoB subunits previously described by others (28). The control plasma VLDL is seen to contain both large and small molecular weight apoB subunits ($apoB_{335K}$ and $apoB_{240K}$). GalN plasma VLDL contained the $apoB_{240K}$ subunit exclusively. A depletion of VLDL $apoB_{335K}$ was observed despite an increase in overall VLDL apoB concentration (Table 2).

HDL_1 from GalN-treated rats appears to have been depleted in apoA-II and apoC peptides, while apoA-I was unaltered (Fig. 1B). The apoE in GalN HDL_2 increased while apoA-I, apoA-II, apoA-IV, and apoC were depleted. Somewhat different results occurred in HDL_3. ApoA-II, apoA-IV, and apoC peptides were depleted (Fig. 1B). As in HDL_1 and HDL_2, apoE was increased in HDL_3 from GalN-treated rats.

Since the $d > 1.21$ g/ml apoprotein content cannot be readily determined by the PAGE technique in the presence of plasma proteins, an estimation of total plasma apoprotein content is not possible. Based on densitometric analysis of stained gels and the analysis of sequentially isolated HDL fractions, we estimate the apoE content of $d > 1.006$ g/ml lipoproteins may be increased by as much as 300%.

Isoelectric focusing of apoA-II, apoC-II, and apoC-III

Equal amounts of protein from VLDL and HDL subfractions were separated by isoelectric focusing in a pH 3.0–6.0 gradient so that the relative content of each apoprotein could be determined. Since apoE and apoA-IV bands co-focus in this system, and apoA-I moves to the extreme basic end of the gel, only the region from pH 4.45 to 5.0, containing apoA-II and apoC proteins is shown.

The isoelectric focusing patterns of apoVLDL and apoHDL shown in **Fig. 2A and B** show that the apoC pattern of VLDL and HDL from GalN rats resemble each other, while control VLDL and HDL patterns are similar. In GalN VLDL, apoC-III_o comprised 2.0% of VLDL apoC peptides as compared to 20.5% in control; apoC-II and apoC-III_3 constituted the majority of the GalN apoC content. These latter peptides are 39.7% and 55.0% of the VLDL apoC's as compared to 27.7% (C-II) and 41.4% (C-III_3) in control VLDL.

ApoA-II was not detected in GalN-treated HDL fractions whereas it was in the control HDL (Fig. 2B). ApoC-III_o was also absent from GalN HDL_1 and HDL_3. A trace of C-III_o was detected in GalN HDL_2. The presence of C-II and C-III_o bands in focused HDL_1, HDL_2, and HDL_3 from GalN-treated plasma is also shown in Fig. 2B.

Effect of GalN treatment on lipoprotein ultrastructure

Electron microscopy of negatively stained lipoprotein fractions isolated by sequential ultracentrifugation was carried out to correlate these fractions with those from density gradients. Control VLDL was uniform while GalN VLDL was heterogeneous, appearing to consist of two populations of particles (**Fig. 3**). The population in greatest abundance in this fraction consisted of very large (diameter = 194.6 ± 48.4) irregularly shaped particles whose edges appear rough and either "notched" or multilamellar. The second population of particles in GalN VLDL appeared similar to control VLDL, being spherical when free-standing or polygons when aggre-

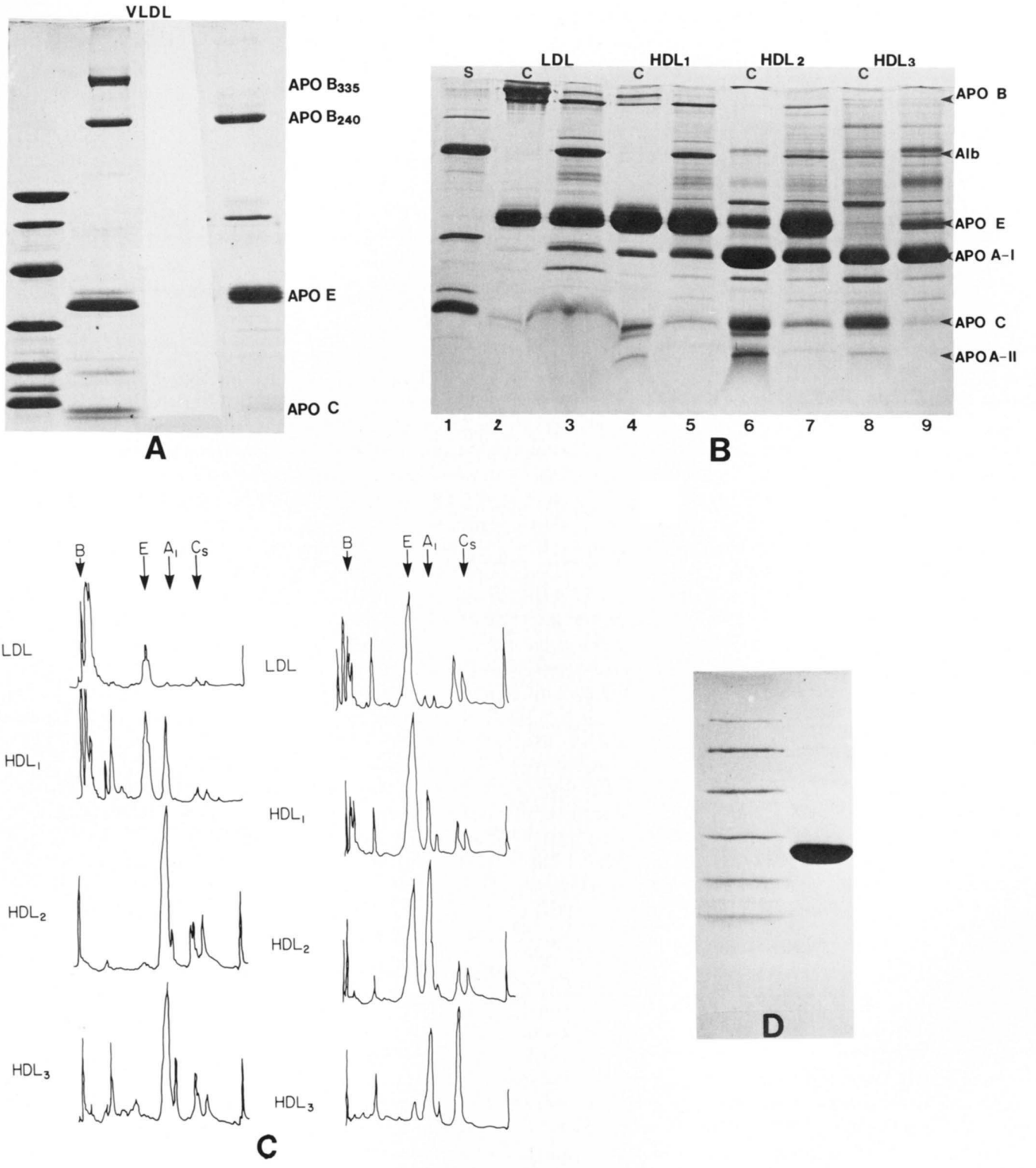

Fig. 1. Discontinuous SDS polyacrylamide gel electrophoretic pattern of apolipoproteins from control rats (left lane of each set) and galactosamine-treated rats (right lane). Fig. 1A shows patterns of apoVLDL; Fig. 1B shows patterns of apoLDL and apoHDL, respectively. Fig. 1C shows densitometer tracings of sliced gels in 1B (control, left; GalN, right). Lane 1 in 1A and 1B shows the migration of molecular weight standards. Fig. 1D shows the migration of purified apoA-I and molecular weight standards. In 1A and 1B, equal amounts (peak column fractions) of apolipoprotein (25 μg) were solubilized in 1% 2-mercaptoethanol and electrophoresed in the presence of 0.1% SDS. Gels are a linear gradient in polyacrylamide ranging from 10% (top) to 20% (bottom) or 3.5 to 27% (1A). The molecular weights of the apoB subunits in the latter gel system have been confirmed in other gels by comparison with proteins of comparable molecular weight.

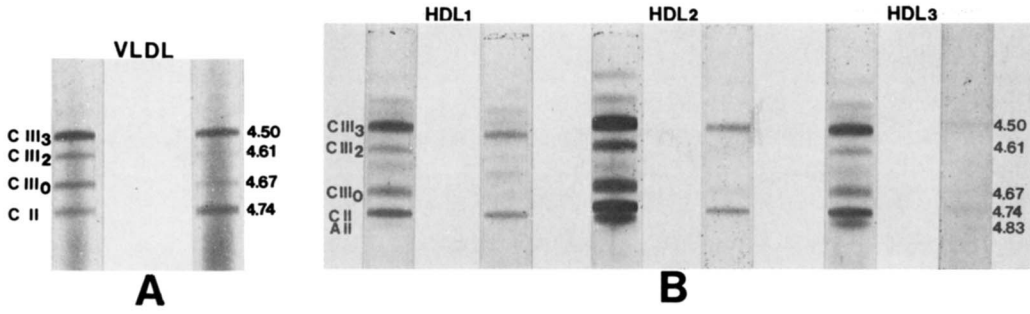

Fig. 2. Isoelectric focusing gels of VLDL (2A) and HDL (2B) from control animals (left lane of each set) and galactosamine-treated animals (right lane). Apoprotein identities are given on the basis of pI values according to Swaney and Gidez (24).

gated. Control VLDL diameter was 69.5 ± 20.3 nm; the smooth-edged spherical particles in GalN VLDL were 63.4 ± 13.2 nm in diameter. Morphologies of LDL and HDL from control and GalN-treated rats were similar to those which we have shown in a previous paper (12); as in that study, d > 1.006 g/ml GalN lipoproteins consisted mainly of flattened vesicular and discoidal structures.

Density gradient analysis of d > 1.006 g/ml lipoproteins from plasma of control and GalN-treated rats (Fig. 4)

Inasmuch as the composition and ultrastructure of sequentially isolated lipoprotein fractions appeared heterogeneous, we employed a separation of d > 1.006 g/ml lipoproteins by centrifugation and tube-slicing fol-

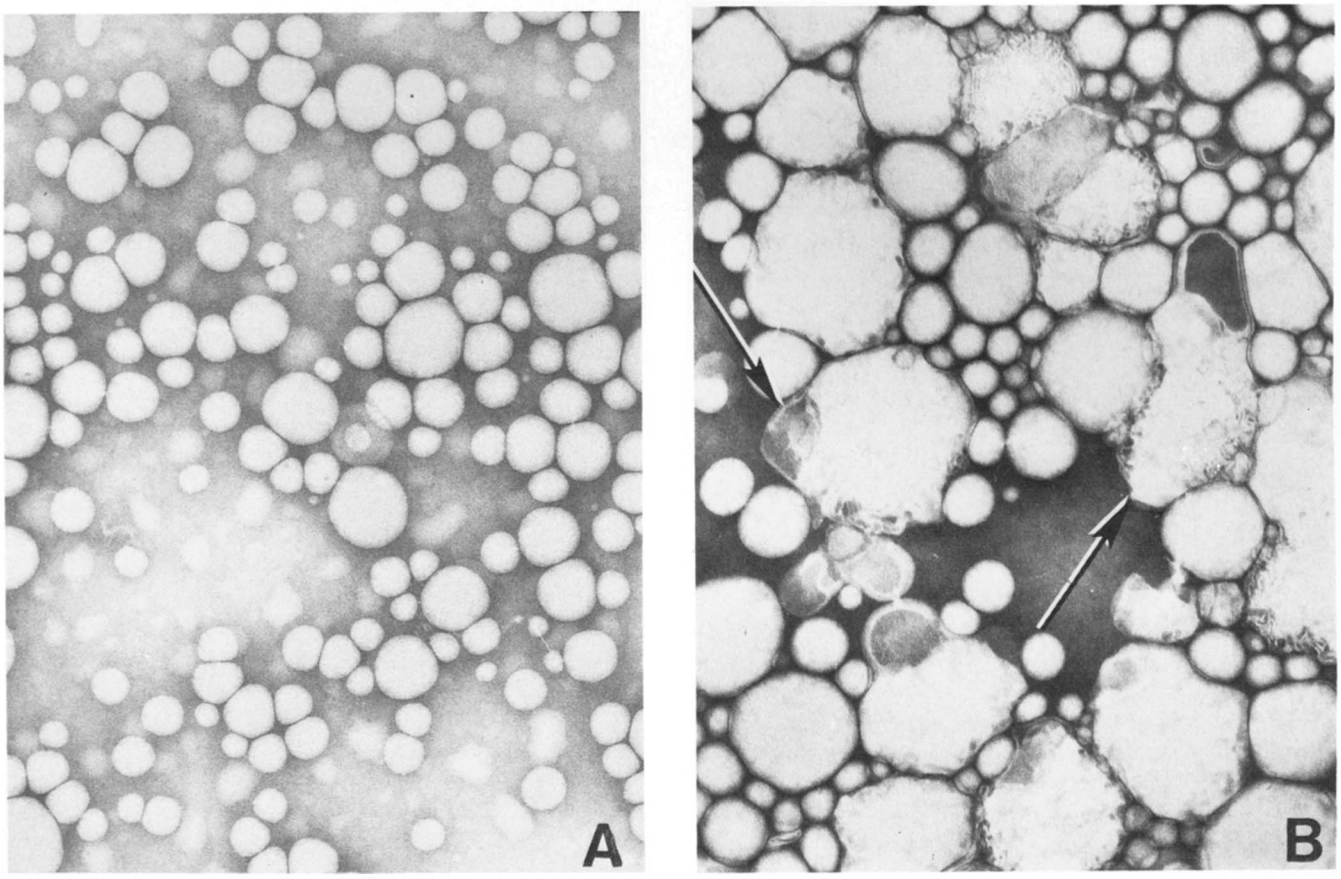

Fig. 3. Electron micrographs of VLDL from control (3A) and galactosamine-treated rats (3B). The arrows in 3B indicate the abnormally large (avg diameter 194.6 ± 48.4 nm) irregularly shaped particles in GalN-treated animals in contrast to control VLDL (avg diameter 69.5 ± 3.2 nm). Final magnification: 100,000×.

lowed by a density gradient fractionation. Our objective in this procedure was to better define the changes in lipoprotein composition and the association of various apoproteins and lipid classes that result from GalN hepatitis.

A unique feature of this gradient is that it is formed with both sucrose and NaBr to decrease ionic strength and assure quantitative recovery of apoprotein and lipid components in gradient fractions. Based on analysis of $d > 1.006$ g/ml fractions before centrifugation and on analysis of gradient fractions, recovery of unesterified cholesterol was 94%, cholesteryl ester 91%, and phospholipid 96%. Apoprotein recoveries in identical density gradients of human samples were 94% (apoA-I) as judged by immunoassay techniques.

Fig. 4 shows the distribution of cholesteryl esters, unesterified cholesterol, and phospholipid in density gradients. The major cholesteryl ester peak in the control gradient is absent in the GalN gradient and the major $d > 1.006$ g/ml lipoproteins are LDL and HDL_1, (fractions 3–8, d 1.028–1.060 g/ml) composed mainly of phospholipid and unesterified cholesterol and, as demonstrated below, most of the apoE (Fig. 5). The broad phospholipid peak seen in fractions 12–20 (d 1.150–1.40 g/ml) in Fig. 4A (control) was unaltered by GalN treatment (Fig. 4B). The material in this density range was lipid-extractable phosphorus and appeared by thin-layer chromatography to contain an appreciable proportion (43–60% by weight) of lysolecithin along with lecithin, phosphatidylethanolamine, and sphingolipids. The observed high proportion of lysolecithin is in agreement with a report of Switzer and Eder (29) that the rat plasma contains a higher proportion of lysolecithin than human plasma, and that a high proportion of the lysolecithin is bound to albumin and is found in the high density fractions of plasma. The predominate protein in fractions 14–20 (d 1.145–1.40 g/ml) of the control gradient detected by PAGE analyses was albumin (see below). We do not presently know the structure of these high density particles.

Distribution of apoproteins in density gradient fractions

Fig. 5 shows the results of PAGE analysis of apoproteins in density gradient fractions. In contrast to sequential fractions, equal volumes, rather than equal amounts of protein from each gradient fraction were electrophoresed. The differences in total dye binding between the various apoprotein bands thus provide a relative quantitation of apoproteins in a range of d 1.006 to 1.175 g/ml (fractions 1–15). An additional feature of these density gradients is that the relative distributions of the various apoproteins in this slab gel system permit conclusions as to specific apoprotein composition. Thus two or more apoproteins may demonstrate an identical gradient profile if associated on a single type of lipopro-

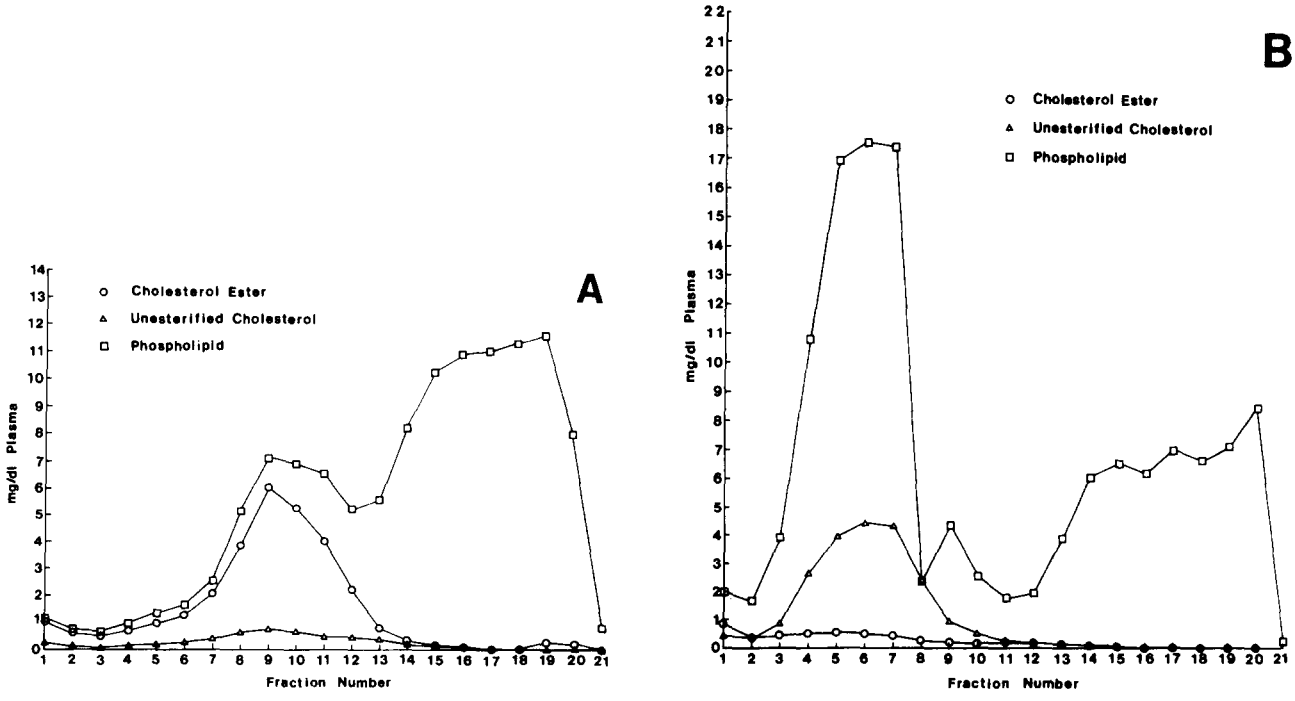

Fig. 4. Distribution of cholesterol, cholesteryl ester, and phospholipid after density gradient separation of $d > 1.006$ g/ml lipoproteins. Results of control (panel A) and galactosamine (panel B) fraction analysis were corrected for dilution during centrifugation and are given as mg/dl plasma.

tein. Analysis of apoproteins in gradient fractions 15–20 (d 1.175–1.40 g/ml) was not possible with this PAGE system because of the high content of albumin.

The increase of apoE in lipoproteins isolated by sequential ultracentrifugation was confirmed in slab gels of density gradient fractions. We did, however, observe a greater number of apoE bands in density gradient fractions than in sequential fractions, though these bands could be observed by increasing the amount of protein loaded on to the slab gel lanes. The distribution of the increased apoE in GalN gradients corresponded well with that of increased gradient phospholipid and unesterified cholesterol shown above.

Differences in apoprotein patterns from similar lipoprotein classes isolated by sequential or density gradient centrifugation are probably caused by the following: *1*) differences in the total amount of protein loaded on the gel; 25 μg of protein was loaded on gels shown in Fig. 1B, while the gels of Fig. 5 contained equal volume aliquots (and hence unequal protein loads) of each density fraction shown; and *2*) the tendency of repeated sequential ultracentrifugations to remove some apolipoproteins more than others (30). Since the density gradient technique involves fewer spins in the ultracentrifuge, it would be expected that apoprotein losses would be less than those from sequentially isolated lipoprotein classes.

As shown in Fig. 5, apoA-I in control density gradient fractions appeared as a single peak (fractions 8–12, d 1.050–1.150 g/ml) corresponding to the cholesteryl ester peak in density gradient profiles (Fig. 4), whereas the apoA-I in GalN density gradient fractions appeared in two peaks at fractions 5 (d 1.038 g/ml) and 6, and at fractions 10–12 (d 1.080–1.150 g/ml). Similar to sequential studies, apoA-IV was depleted in GalN gradient fractions and had an apparent redistribution from HDL to LDL particles.

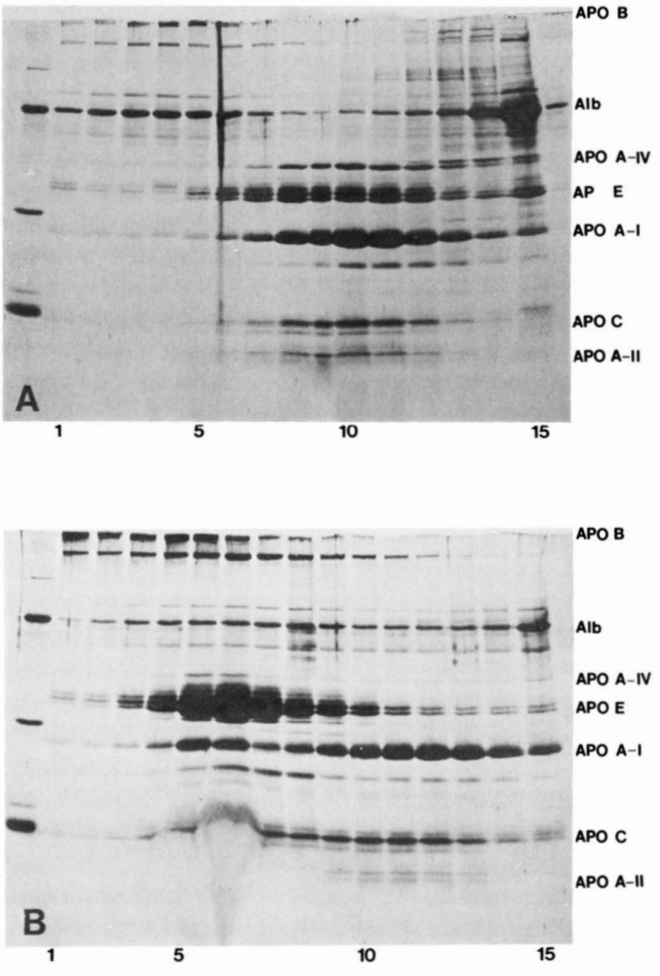

Fig. 5. SDS polyacrylamide gel electrophoretic separation of apoproteins in gradient fractions 1 through 15. Fractions from control rat (panel A) and galactosamine-treated rat (panel B) of d > 1.006 g/ml lipoprotein gradients were electrophoresed as in Fig. 1 using equal volumes (35 μl) of gradient fractions. The far left lane in each slab shows the migration of molecular weight standards and lane numbers correspond to gradient fraction numbers.

Effects of GalN treatment on ultrastructure of d > 1.006 g/ml lipoproteins in density gradient fractions

Fig. 6 shows electron micrographs of lipoproteins in density gradient fractions after dialysis and negative staining. The predominant lipoproteins in the GalN gradient are discoidal, pseudomicellar, and flattened vesicular structures, while only spherical particles are seen in the control gradient. There is an apparent decreased number of rouleaux in density gradient fractions relative to sequentially isolated fractions (12), suggesting that their formation may be artifactual. In this density gradient the following fractions correspond to sequential fractions: LDL, 1 through 6; HDL_1, 7 through 9; HDL_2, 10 through 13; and HDL_3, 14 through 17.

As shown in Fig. 6, GalN gradients contain discoidal structures, predominately in rouleaux, a variety of spherical particles in the LDL size range, and some aggregates, probably formed during the negative stain procedure. In fractions corresponding to HDL_1 there are a mixture of large aggregates as well as uniform particles which either form rouleaux or appear as single discs. The average diameter of these smaller discs is similar to that of sequential HDL_1 and to nascent HDL isolated by others with liver perfusion systems (6). These particles are particularly abundant in fraction 8 (d 1.050 g/ml). Similarly, HDL_2 in the GalN gradient appears either as large irregularly shaped aggregates or as small discoidal structures which are single discs or clusters. The average diameter of these discs is 12.7 ± 5.1 nm and the thickness is 5.1 ± 3.7 nm.

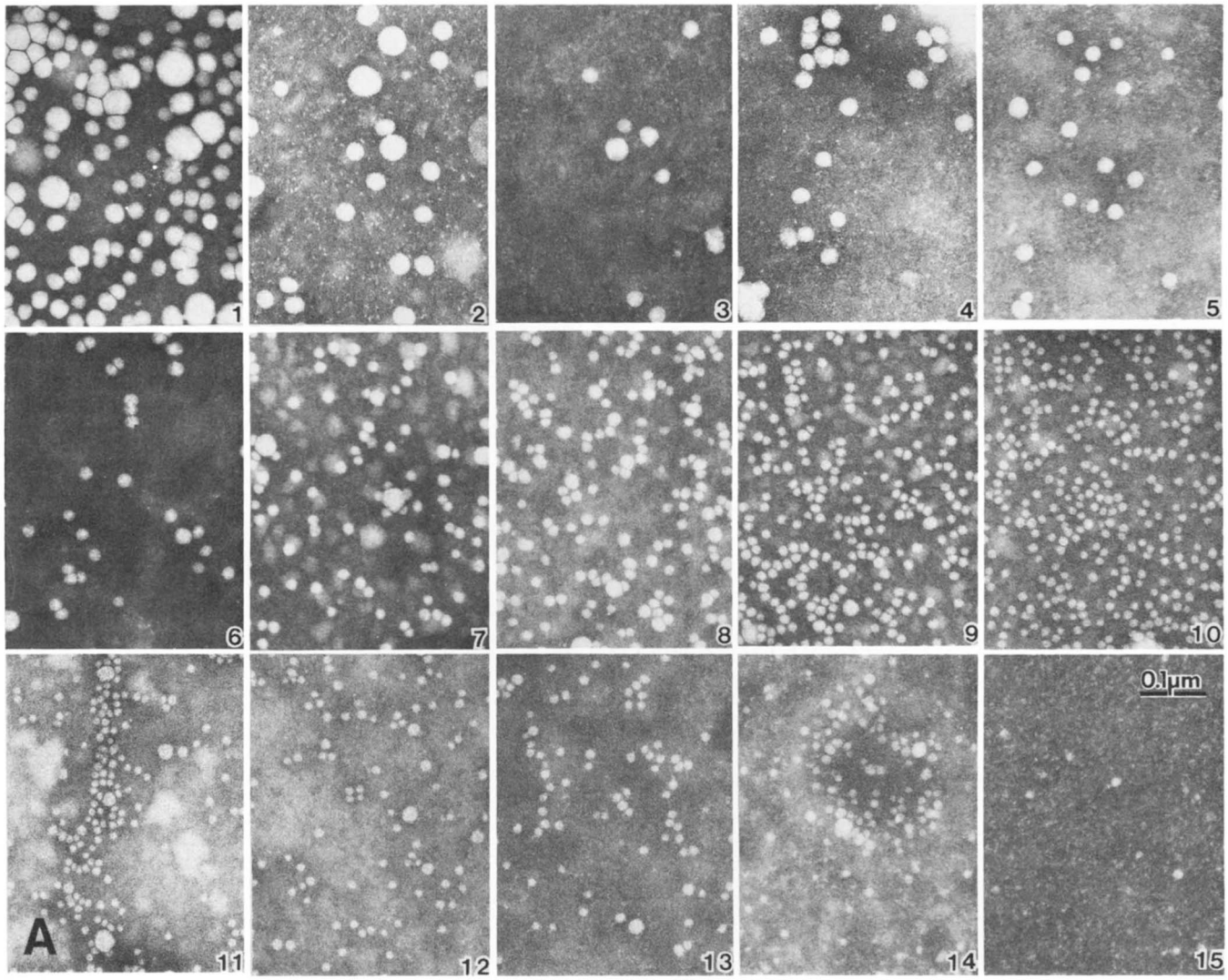

Fig. 6. Electron micrographs of control (panel A) and galactosamine (panel B) density gradient fractions. Gradient fractions were dialyzed against 1 mM EDTA, 0.02% sodium azide, and uniformly stained with 2% phosphotungstate (see text). Photograph numbers correspond to gradient fraction numbers.

As with the sequentially isolated GalN HDL_3, density gradient fractions 14 and 15 contain few particles. We observed more spherical particles in these fractions (average diameter 7.9 ± 2.3 nm) and a few discs similar to those observed in lighter density gradient fractions and sequentially isolated HDL_2.

DISCUSSION

Previous studies from this laboratory have shown that GalN-induced hepatitis in rats is associated with increased plasma levels of unesterified cholesterol, phospholipid, and triglyceride, severe plasma LCAT deficiency, and the appearance of discoidal lipoproteins in plasma (12, 13).

This report extends these studies by determining the optimum conditions for inducing this cholesterol esterification defect, by determining the apoprotein changes in plasma lipoproteins, and by correlating lipoprotein morphology with apoprotein and lipid content of lipoproteins isolated by either sequential or density gradient ultracentrifugation. Our results show that GalN hepatitis results in an apparent decrease in apoC and an increase in triglyceride and apoB content of VLDL, while unesterified cholesterol and phospholipid accumulate in LDL and HDL whose content of apoE appears enhanced. These alterations in composition are reflected in altered lipoprotein morphology.

We have confirmed the work of others that normal rat plasma VLDL contains the $apoB_{335K}$ and $apoB_{240K}$ subunits (28). However, we find that the larger $apoB_{335K}$

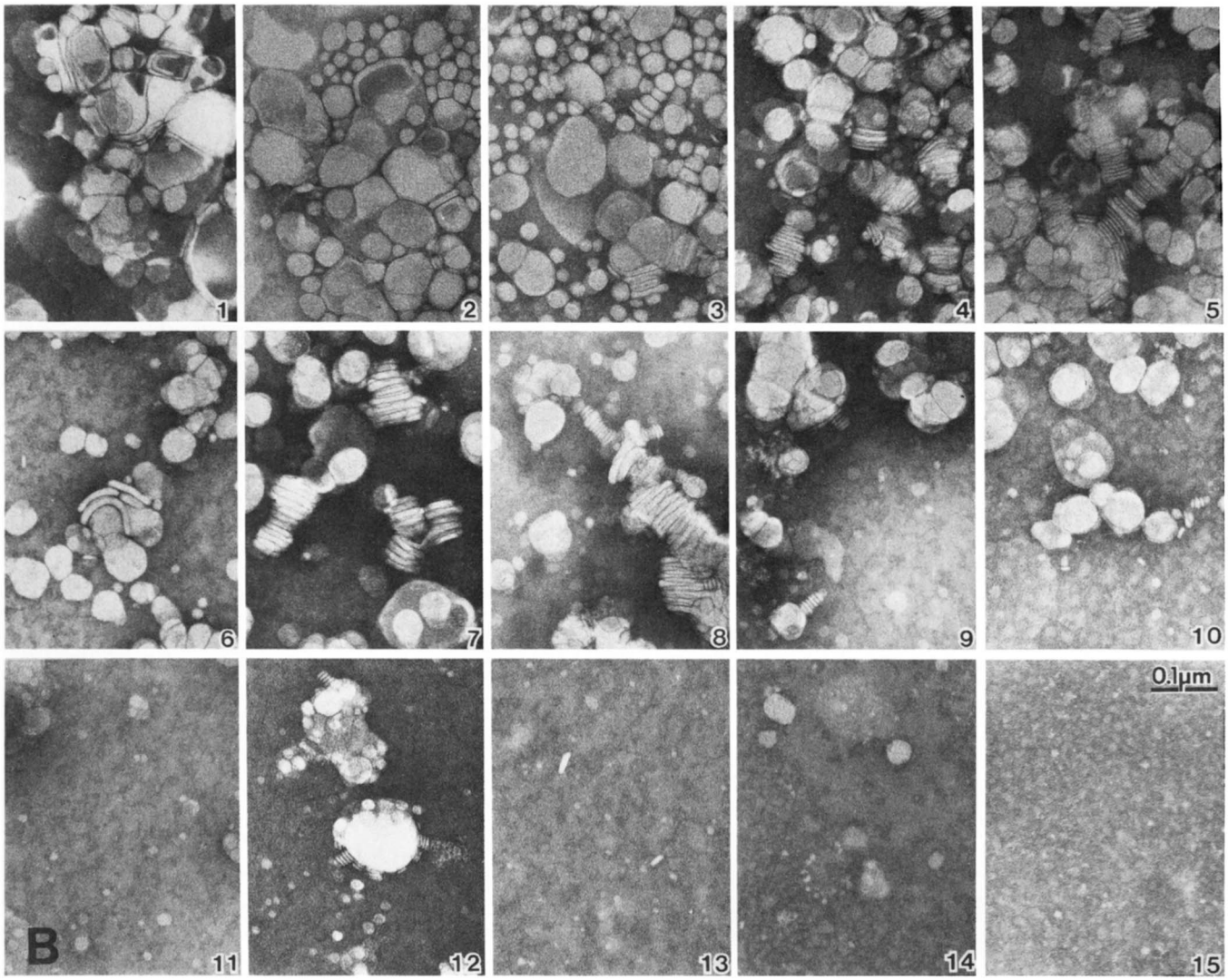

Fig. 6. (*Continued*)

subunit is greatly diminished in GalN rat plasma VLDL. Other workers have found that the liver secretes both apoB subunits while the intestine secretes only the small subunit (28). Therefore, GalN-induced liver injury appears to affect synthesis and/or secretion of the larger apoB subunit by the liver. Further studies into the mechanism of the decrease in $apoB_{335K}$ in GalN-treated rats are presently underway.

Sirowej and Katterman (31) have reported that all apoC proteins were diminished in both VLDL and HDL by GalN treatment. Our results indicate diminishment of only $apoC\text{-}III_0$ and $apoC\text{-}III_2$ in apoVLDL of GalN-treated rats, while all apoC proteins appear to be decreased in the HDL subspecies. These investigators (31), using a lower dose of GalN, also detected no change in the apoA-I or apoE content of HDL after GalN treatment. We have demonstrated that cholesteryl ester levels are related to the dose of GalN and that the change in the apoE:apoA-I ratio is proportional to decreased cholesteryl ester content, a reflection of possible decreased LCAT activity. Thus, selection of affected animals solely on the basis of α-lipoprotein deficiency, as used by Sirowej and Katterman (31), does not adequately select animals with maximum LCAT deficiency.

The morphology and ultrastructure of many of the d > 1.006 g/ml lipoproteins in this study bear close resemblance to a similar fraction from humans with familial LCAT deficiency (32), while many HDL particles appear similar to nascent HDL found by Hamilton and co-workers (6) in rat liver perfusates in the presence of the LCAT inhibitor DTNB. In perfusion studies, HDL was rich in unesterified cholesterol and phospholipid and appeared as discoidal particles when viewed by electron microscopy. Addition of DTNB to the perfusion medium

increased the concentration of these lipids in HDL, increased the HDL apoE:apoA-I ratio, and increased LCAT reactivity over that of plasma HDL. Similarly, Marsh (3) showed that newly secreted HDL was richer in unesterified cholesterol and phospholipid than serum HDL, and that perfusate HDL was richer in apoE than serum HDL. Felker et al. (32) have found that the relative amounts of apoA-I and apoE recovered from liver perfusates were a function of the extent to which LCAT was inhibited during perfusion and suggested an inverse relationship between perfusate cholesteryl ester content and apoE in nascent HDL in rats. This implies that the liver secretes less apoA-I if LCAT is inhibited, or that apoA-I is secreted but not incorporated into HDL as a result of LCAT inhibition. The HDL in our studies may also represent unmetabolized secretory forms of HDL, particularly since the apoprotein composition of the discoidal HDL is similar to the nascent HDL obtained from rat liver perfusates.

Lipoprotein abnormalities in the GalN-induced LCAT deficiency and similar changes in familial LCAT deficiency (10, 33, 34) and in patients with liver disease (7–9, 11) clearly emphasize the central role of LCAT in plasma lipoprotein metabolism. Thus apoE, cholesterol, and phospholipid-rich lipoproteins may represent the principle form in which cholesterol is secreted by the liver and, in the presence of LCAT, may be the source of the apoE and cholesteryl ester of plasma VLDL. Investigations by Ragland et al. (7) and Marcel et al. (9) using plasma from alcoholic hepatitis patients and by Mitchell et al. (10) with familial LCAT-deficient patients have demonstrated the presence of unesterified cholesterol, phospholipid, and apoE-rich HDL which, in all three studies, proved to be a better LCAT substrate than plasma HDL. The accumulation in plasma of such a species has thus been suggested to be substrate accumulation due to LCAT deficiency. In the present study similar particles appear to occur in plasma during GalN-induced LCAT deficiency and may also represent LCAT substrate accumulation due to decreased hepatic LCAT synthesis or secretion.

Discoidal and multilamellar lipoproteins have been observed in in vitro experiments using phospholipid or phospholipid–cholesterol unilamellar vesicles mixed with whole rat plasma, serum lipoproteins, albumin, or purified lipoproteins (35). In these in vitro experiments the conversion of spherical phospholipid vesicles to discoidal lipoprotein complexes released the vesicle contents and this release was attributed to the apoE or apoA-I content of these mixtures. The mechanism of formation of discoidal lipoproteins in plasma remains obscure and, since discoidal structures are not visualized in hepatocyte Golgi, one explanation for the structures we observe is that they may be formed after secretion. Thus, we are unsure as to whether the marked increase in apoE-rich lipoproteins represents the accumulation of secretory lipoproteins due to decreased LCAT activity, or whether these species might be the result of increased hepatic secretion of apoprotein-free lipid vesicles that acquire apoprotein from other lipoproteins or from unbound plasma pools after secretion. An increased hepatic secretion of such vesicles might well be the result of GalN-induced cholestasis secondary to the hepatocellular injury.

The results reported here extend our knowledge of the composition of abnormal lipoproteins that accumulate in plasma during LCAT deficiency and may demonstrate the accumulation of nascent lipoproteins in an intact animal. Furthermore, the present results clearly show that the discoidal apoE-rich particles isolated by others from perfused liver systems are not artifacts of the perfusion technique since they are similar to the particles observed in vitro and in vivo. The possibility that nascent lipoproteins may accumulate in plasma during GalN hepatitis in large quantities could prove fruitful in further studies of nascent lipoprotein metabolism.

We are, at present, pursuing the metabolic fate and synthesis rates of lipids, apoE, and apoA-I in GalN-treated animals. The results of these experiments may provide a better understanding of the role of the apoE-rich nascent lipoprotein metabolic pathway.

We greatly appreciate the skilled assistance of Lois Kuiken, Sharon Frase, Barbara Mays, and Jim Case. We also gratefully acknowledge the help of Dr. Patrick Tso with the thin-layer chromatographic separation of phospholipids and Dr. Neil Manowitz with resolution of the VLDL apoB subunits by SDS-PAGE. This research was supported by research grants from the National Institutes of Health HL 23945-08 and NIH 5T32 AM 07292 and (in part) by an award from the UTCHS New Faculty Research Grant Program.

Manuscript received 17 March 1981, in revised form 12 August 1981, and in re-revised form 4 January 1982.

REFERENCES

1. Wu, A. L., and H. G. Windmueller. 1979. Relative contributions by liver and intestine to individual plasma apolipoproteins in the rat. *J. Biol. Chem.* **254:** 7316–7322.
2. Shaefer, E. J., S. Eisenberg, and R. I. Levy. 1978. Lipoprotein apoprotein metabolism. *J. Lipid Res.* **19:** 667–686.
3. Marsh, J. B. 1974. Lipoproteins in a nonrecirculating perfusate of rat liver. *J. Lipid Res.* **15:** 544–550.
4. Osborne, J. C., Jr., and H. B. Brewer, Jr. 1977. The plasma lipoproteins. *Adv. Protein Chem.* **31:** 253–337.
5. Tall, A. R., P. H. Green, R. M. Glickman, and J. W. Riley. 1979. Metabolic fate of chylomicron phospholipids and apoproteins in the rat. *J. Clin. Invest.* **64:** 977–989.
6. Hamilton, R. L., M. C. Williams, C. J. Fielding, and R. J. Havel. 1976. Discoidal bilayer structure of nascent high density lipoproteins from perfused rat liver. *J. Clin. Invest.* **58:** 667–680.

7. Ragland, J. B., P. D. Bertram, and S. M. Sabesin. 1978. Identification of nascent high density lipoproteins containing arginine-rich protein in human plasma. *Biochem. Biophys. Res. Commun.* **80:** 81–88.
8. Ragland, J. B., C. Heppner, and S. M. Sabesin. 1978. The role of LCAT deficiency in the apoprotein metabolism of alcoholic hepatitis. *Scand. J. Clin. Lab. Invest.* **38:** 208–213.
9. Marcel, Y. L., C. Vézina, D. Emond, and G. Suzue. 1980. Heterogeneity of human high density lipoprotein: presence of lipoproteins with and without apoE and their roles as substrates for lecithin:cholesterol acyltransferase reaction. *Proc. Natl. Acad. Sci. USA.* **77:** 2969–2973.
10. Mitchell, C. D., W. C. King, K. R. Applegate, T. Forte, J. A. Glomset, K. R. Norum, and E. Gjone. 1980. Characterization of apolipoprotein E-rich high density lipoproteins in familial lecithin:cholesterol acyltransferase deficiency. *J. Lipid Res.* **21:** 625–634.
11. Sabesin, S. M., H. L. Hawkins, L. Kuiken, and J. B. Ragland. 1977. Abnormal plasma lipoproteins and lecithin:cholesterol acyltransferase deficiency in alcoholic liver disease. *Gastroenterology.* **72:** 510–518.
12. Sabesin, S. M., L. B. Kuiken, and J. B. Ragland. 1975. Lipoprotein and lecithin:cholesterol acyltransferase changes in galactosamine-induced rat liver injury. *Science.* **190:** 1302–1304.
13. Sabesin, S. M., L. B. Kuiken, and J. B. Ragland. 1978. Lipoprotein abnormalities in galactosamine hepatitis: a model of experimental LCAT deficiency. *Scand. J. Clin. Lab. Invest.* **38:** 187–193.
14. Lindgren, F. T. 1975. Preparative ultracentrifugal laboratory procedures and suggestions for lipoprotein analysis. *In* Analysis of Lipid and Lipoproteins. E. G. Perkins, editor. Amer. Oil Chem. Soc. 204–224.
15. Biggs, H. G., J. M. Erickson, and W. R. Moorehead. 1975. A manual colorimetric assay of triglycerides in serum. *Clin. Chem.* **21:** 437–441.
16. Blomhoff, J. P. 1973. Serum cholesterol determination by gas–liquid chromatography. *Clin. Chem. Acta.* **43:** 257–265.
17. Rouser, G., S. Fleischer, and A. P. Yamamoto. 1969. Two-dimensional thin-layer chromatographic separation of polar lipids and determination of phospholipids by phosphorus analysis of spots. *Lipids.* **5:** 494–496.
18. Markwell, M. K., S. M. Haas, L. L. Bieber, and N. E. Tolbert. 1978. A modification of the Lowry procedure to simplify protein determination in membrane and lipoprotein samples. *Anal. Biochem.* **87:** 206–210.
19. Laemmli, U. K. 1970. Cleavage of structural proteins during the assembly of the head of bacteriophage T4. *Nature.* **222:** 680–685.
20. Weber, K., and M. Osborne. 1969. The reliability of molecular weight determinations by dodecyl sulfate-polyacrylamide gel electrophoresis. *J. Biol. Chem.* **244:** 4406–4412.
21. Holmquist, L., K. Carlson, and L. A. Carlson. 1978. Comparison between the use of isopropanol and tetramethylurea for the solubilization and quantitation of human serum very low density apolipoproteins. *Anal. Biochem.* **88:** 457–460.
22. Fainaru, M., R. J. Havel, and T. E. Felker. 1977. Radioimmunoassay of apolipoprotein A-I of rat serum. *Biochim. Biophys. Acta.* **446:** 56–68.
23. Weidman, S. W., B. Suarez, J. M. Falko, J. C. Witztum, J. Kolar, M. Raben, and G. Schonfeld. 1979. Type III hyperlipoproteinemia: development of a VLDL apoE gel isoelectric focusing technique and application in family studies. *J. Lab. Clin. Med.* **93:** 549–569.
24. Swaney, J. B., and L. I. Gidez. 1977. Analysis of rat serum apolipoproteins by isoelectric focusing. II. Studies on the low molecular weight subunits. *J. Lipid Res.* **18:** 69–76.
25. Forte, T., and A. V. Nichols. 1972. Application of electron microscopy to the study of plasma lipoprotein structure. *Adv. Lipid Res.* **10:** 1–41.
26. Decker, K., and D. Keppler. 1972. Galactosamine-induced liver injury. *Prog. Liver Dis.* **4:** 183–199.
27. Sabesin, S. M., and J. B. Ragland. 1978. Role of free fatty acids in the pathogenesis of fatty liver. *Exp. Mol. Pathol.* **29:** 82–91.
28. Krishnaiah, K. V., L. F. Walker, J. Borensztajn, G. Schonfeld, and G. S. Getz. 1980. Apolipoprotein B variant derived from rat intestine. *Proc. Natl. Acad. Sci. USA.* **77:** 3806–3810.
29. Switzer, S., and H. A. Eder. 1965. Transport of lysolecithin by albumin in human and rat plasma. *J. Lipid Res.* **6:** 506–511.
30. Fainaru, M., R. J. Havel, and K. Imaizumi. 1977. Apoprotein content of plasma lipoproteins of the rat separated by gel chromatography or ultracentrifugation. *Biochem. Med.* **17:** 347–355.
31. Sirowej, H., and R. Katterman. 1978. Apolipoproteins of rats treated with D-galactosamine. *Hoppe-Seyler's Z. Physiol. Chem.* **359:** 1443–1445.
32. Felker, T. E., M. Fainaru, R. L. Hamilton, and R. J. Havel. 1977. Secretion of the arginine-rich and A-I lipoproteins by the isolated perfused rat liver. *J. Lipid Res.* **18:** 465–473.
33. Glomset, J. A., K. Applegate, T. Forte, W. C. King, C. D. Mitchell, K. R. Norum, and E. Gjone. 1980. Abnormalities in lipoproteins of d < 1.006 g/ml in familial lecithin:cholesterol acyltransferase deficiency. *J. Lipid Res.* **21:** 1116–1127.
34. Forte, T., K. R. Norum, J. A. Glomset, and A. V. Nichols. 1971. Plasma lipoproteins in familial lecithin:cholesterol acyltransferase deficiency: structure of low and high density lipoproteins as revealed by electron microscopy. *J. Clin. Invest.* **50:** 1141–1148.
35. Guo, L. S. S., R. L. Hamilton, J. Goerke, J. N. Weinstein, and R. J. Havel. 1980. Interaction of unilamellar liposomes with serum lipoproteins and apolipoproteins. *J. Lipid Res.* **21:** 993–1003.